Autonomous resonant frequency tuning controller for repeater resonator in resonant inductive coupling wireless power transfer system

Akihiro Konishi, Kazuhiro Umetani, Masataka Ishihara, and Eiji Hiraki

Graduate school of natural science and technology,
Okayama University,
Okayama, Japan

Published in: 2021 IEEE 30th International Symposium on Industrial Electronics (ISIE)

DOI: 10.1109/ISIE45552.2021.9576268

Autonomous Resonant Frequency Tuning Controller for Repeater Resonator in Resonant Inductive Coupling Wireless Power Transfer System

Akihiro Konishi
Okayama University
Graduate School of Natural Science and Technology
Okayama, Japan
p3448o58@s.okayama-u.ac.jp

Kazuhiro Umetani
Okayama University
Graduate School of Natural Science and Technology
Okayama, Japan
umetani@okayama-u.ac.jp

Masataka Ishihara
Okayama University
Graduate School of Natural Science and Technology
Okayama, Japan
masataka.ishihara@okayama-u.ac.jp

Eiji Hiraki
Okayama University
Graduate School of Natural Science and Technology
Okayama, Japan
hiraki@okayama-u.ac.jp

***Abstract*— The resonant inductive coupling wireless power transfer technique (RIC-WPT) is emerging as a promising wireless power transfer method for small mobile devices with comparatively high-power transfer capability and good efficiency. However, the performance of the RIC-WPT system is severely deteriorated by the resonant frequency detuning of the transmitter, repeater, and receiver resonators, which can be naturally caused by the manufacturing tolerance and the aging effect of these resonators. Particularly, the detuning of the repeater resonator tends to severely affect the performance due to its high-quality factor, which should be solved for practical application of RIC-WPT technology. This paper addresses this difficulty by proposing an autonomous resonant frequency tuning controller circuit for the repeater resonator. The controller tunes the resonant frequency of the repeater resonator to the operating frequency of the inverter, driving the transmitter, without an external power supply and wireless communication with the inverter controller, which restricts the freedom of the installation location and therefore preferably be avoided in the wireless power transfer system. The operating principles of the proposed controller were confirmed by the circuit simulator, supporting the feasibility of the proposed controller.**

Keywords— Control circuit, Frequency Synchronization, Hill climbing method, Resonant frequency, Wireless power transfer

I. INTRODUCTION

The recent progress of the Internet-of-Thing technology is giving rise to the small mobile information devices for industrial, medical, and consumer use. For example, the active radio frequency identification tags (RFID tags) [1][2] and smart sensors [3][4] are increasingly utilized in manufacturing factories and warehouses. The cutting-edge medical examination often involves capsule endoscopy [5][6]; the biomedical implants [7][8] are appearing as a useful tool for medical treatment. In our daily life, smartphones and tablet devices are becoming indispensable for personal communication and entertainment. However, the near-future widespread of these IoT devices incur the need for the power supply method to these devices distributed in a large volumetric area because the cable connection to many small IoT devices will significantly impair the convenience.

The wireless power transfer (WPT) technology is attracting the researchers' attention as a promising technology for this need because this technique enables the simultaneous power supply to many distributed devices without a cable connection. This technology has some different methods. However, the resonant inductive coupling wireless power transfer (RIC-WPT) technique [9]–[13] is a promising candidate owing to its comparatively high power transfer capability at comparatively high efficiency.

Figure 1 illustrates a basic configuration of the RIC-WPT system. This system includes the three coils used for the power transfer via magnetic field: the transmitter coil, the repeater coil, and the receiver coil. Each of these three coils is connected to the resonant capacitor to form the LC resonator, which is designed to have the same resonant frequency. The transmitter resonator is supplied with the ac power at its resonant frequency using the high-frequency inverter, generating the large resonant current flowing through the transmitter coil. This resonant current generates the high-frequency ac magnetic field around the transmitter coil, which causes the voltage induction and induces the large resonance current inside the repeater resonator. The repeater resonator, therefore, generates the ac magnetic field around the repeater

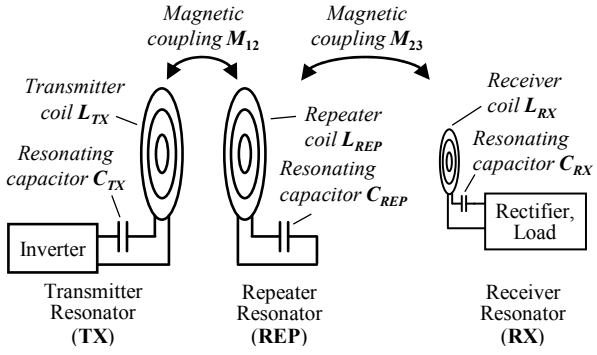

Fig. 1. Basic configuration of resonant inductive coupling wireless power transfer system with repeater resonator.

978-1-7281-9023-5/21/$31.00 ©2021 IEEE

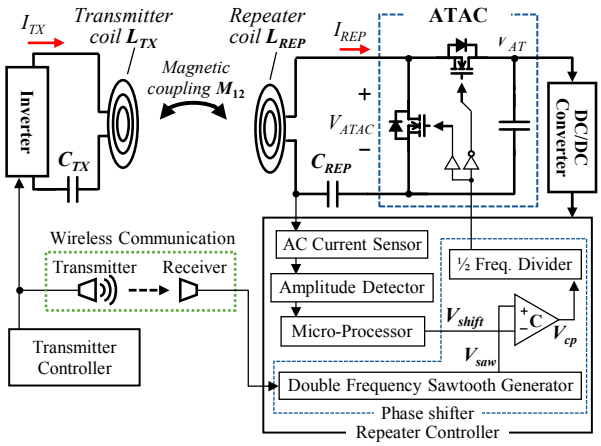

Fig. 2. Previous resonant frequency tuning system of the repeater resonator.

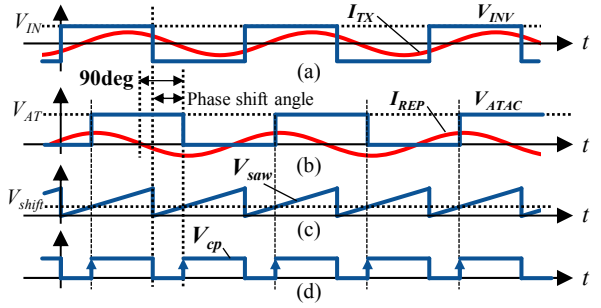

Fig. 3. Operation waveforms of previous resonant frequency tuning system. (a) Inverter output voltage V_{INV} and transmitter coil current I_{TX}. (b) Repeater coil current I_{REP} and ac voltage generated by ATAC V_{ATAC}. (c) Sawtooth wave V_{saw} with the twice as high frequency as the received signal. (d) Square wave V_{cp} with twice as high frequency as the received signal.

coil, thus contributing to expanding the region of the ac magnetic field, i.e. the region for the WPT. Then, the resonant current is induced by the voltage induction in the receiver coil, located in the region of the ac magnetic field. Finally, the dc power can be extracted in the receiver by rectifying the resonant current of the receiver resonator.

According to the operation principles of the RIC-WPT system, these resonators should ideally have the identical resonant frequency for effective generation of the resonant current and efficient power transfer to the receiver. However, in the practical application, the resonant frequency is detuned from the ideal value due to the manufacturing tolerance and the aging effect, which deteriorates the maximum possible power to be transferred. The manufacturing tolerance and the aging effect have a non-negligible effect on the resonant frequency detuning considering that the many commercial inductors and capacitors have the maximum tolerance of 10%, which implies the deviation of the resonant frequency by 10% at maximum. Particularly, the repeater resonator generally has a high quality factor of the resonance due to its simple structure and can easily cause the frequency splitting phenomenon [14]–[20]. Therefore, the repeater resonator tends to suffer from extremely high susceptibility to the detuning, thus hindering the practical application of the RIC-WPT system considering the difficulty of the mass production.

A possible remedy for this problem of the repeater resonator is to develop the autonomous resonance frequency tuning system. For this purpose, many preceding studies have proposed the methods to directly or equivalently tune the resonance frequency of the LC resonator. For example, [16] utilized a variable capacitor as the resonant capacitor and mechanically adjusted the capacitance using the stepping motor. Although this study proved the effective tuning of the resonance frequency, this method leads to large power consumption for tuning the resonant frequency, which also deteriorates the power transfer capability of the RIC-WPT system. To overcome this difficulty, many studies [18], [19], [21]–[23] have proposed the lossless switching circuits that can equivalently adjust the capacitance of the resonant capacitor. These switching circuits are controlled to generate the reactive voltage for compensating the reactive voltage of the LC resonator caused by the detuning of the resonant frequency. Many of these switching circuits need complicated control systems with complicated switching patterns requiring accurate duty ratio or switching timing, which hinders application to high-frequency applications like the RIC-WPT system. However, the Automatic Tuning Assist Circuit (ATAC) [18], [19], [21], [24], [25] was reported to be possibly controlled using a simple control circuit and simple switching pattern, which is attractive for the RIC-WPT system, although preceding studies have not proposed the practical control system of the ATAC for the repeater resonator of the RIC-WPT system.

The purpose of this paper is to propose an autonomous resonant frequency tuning system of the repeater resonator in the RIC-WPT by developing a control circuit of the ATAC. The proposed tuning system is constructed based on the recent studies, in which the feasibility of the tuning system for the repeater resonator using the ATAC was first discussed in [18] and a tuning system using the ATAC was proposed to adjust the resonant frequency of the repeater resonator in [25]. However, the tuning system of [25] was not convenient for practical application because this previous system needed wireless communication with the controller of the transmitter resonator, which restricts the freedom of installation location of the repeater resonator. Therefore, the proposed tuning system was developed such that it operates fully autonomously without an external power supply and wireless communication with the inverter controller of the transmitter.

The remainder of this paper is divided into four sections. Section II briefly reviews the operation principle of the previously proposed tuning system of the repeater resonator including the brief introduction of the ATAC. Section III proposes the novel tuning system and presents its operating principle. Then, section IV shows the simulation results to confirm the operation of the proposed tuning system. Finally, section V gives the conclusions.

II. Review of Previous Resonant Frequency Tuning System of Repeater Resonator

Figure 2 illustrates the previous tuning system proposed in [25]. This figure omits the receiver resonator for simplification. As this paper targets the wireless power transfer to the small IoT devices, the receiver resonator is assumed to receive small power compared with the electric power stored in the transmitter and repeater resonators and therefore the receiver resonator can be regarded to have a negligible effect on the operation of the repeater resonator, as is similar to the discussion in [26]. The resonant frequency of the repeater resonator is assumed to be detuned from the operating frequency of the inverter that drives the transmitter resonator.

The repeater resonator is made of the series connection of the repeater coil, the resonant capacitor, and the ATAC. The ATAC is made of the half-bridge circuit of the switching power devices and the decoupling capacitor that stabilizes the voltage of the half-bridge circuit. The voltage stored in the decoupling capacitor is utilized to compensate for the reactive voltage of the LC resonator of the repeater coil and the resonant capacitor, which should have vanished if the resonant frequency is appropriately tuned. Additionally, a small portion of the dc power stored in the decoupling capacitor is converted into the dc power supply to the controller of the ATAC using the DC/DC converter so that this tuning system can operate without an external power supply.

The half-bridge circuit of the ATAC is operated with the duty cycle of 50% at the same frequency as the inverter of the transmitter, as shown in the operating waveform depicted in Fig. 3(b). The controller of the ATAC adjusts the phase difference between the output voltage of the half-bridge circuit and the transmitter coil current so that the resonant current inside the repeater resonator is maximized. For this purpose, the controller of the ATAC receives the square wave signal synchronizing the polarity of the transmitter coil current or more indirectly the inverter's gate switching signal from the controller of the transmitter via wireless communication. (The phase difference between the inverter output voltage and the transmitter coil current is assumed to be sufficiently stable.) Then, the controller of the ATAC generates the gating signals of the half-bridge circuit by delaying the received signal with an appropriate phase shift angle, which is searched by the ATAC controller to maximize the resonance current in the repeater resonator.

The important function of the ATAC is that it automatically adjusts the ac current flowing into the ATAC to have the phase angle perpendicular to the gating signal of the ATAC by applying an appropriate reactive voltage to the repeater resonator. Noting that the resonant current in the repeater resonator has the same frequency as the inverter that drives the transmitter, the ATAC operates at the same operating frequency as the repeater's resonant current flowing into the ATAC and therefore generates the ac voltage with the same frequency as the resonant current at the input of the ATAC. Remembering that the duty cycle of the half-bridge circuit is 50%, the root-mean-square value of the fundamental wave V_{ATAC} of this ac voltage is expressed as

$$|V_{ATAC}| = \frac{\sqrt{2}}{\pi} V_{AT} \tag{1}$$

where V_{AT} is the dc voltage stored in the decoupling capacitor C_A of the ATAC. Therefore, the equivalent circuit of the repeater resonator, excluding the controller, can be expressed as Fig. 4, where V_{IND} is the ac voltage induced in the repeater coil; C_{REP} is the capacitance of the resonant capacitor; L_{REP} and R_{REP} are the inductance and the ac resistance of the repeater coil, respectively.

According to this equivalent circuit, the ATAC receives the active power $\mathrm{Re}(V_{ATAC}I_{REP}^*)$, where the I_{REP}^* is the complex conjugate of I_{REP}. However, the ATAC cannot receive the active power in the steady-state because the ATAC is made of only passive components except for the switching power devices and therefore is lossless circuit. (The power consumption of the controller of the ATAC is small and

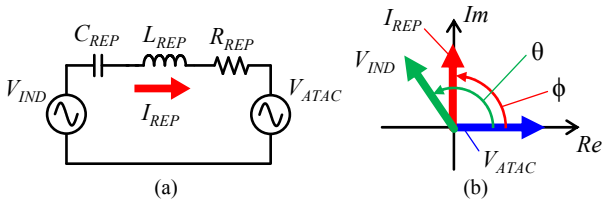

Fig. 4. Equivalent circuit and phase diagram of repeater resonator with ATAC. (a) Equivalent circuit. (b) Phase diagram.

therefore neglected.) This indicates that I_{REP} must be perpendicular to V_{ATAC} in the steady-state.

Next, Kirchhoff's voltage law is considered for this equivalent circuit. If the origin of the phase angle is taken such that the phase angle of V_{ATAC} is zero, Kirchhoff's voltage law can be expressed as the following two equations, which represents the components parallel and perpendicular to V_{ATAC}:

$$|V_{IND}|\cos\theta - |V_{ATAC}| = -\omega\left(L_{REP} - \frac{1}{\omega^2 C_{REP}}\right)|I_{REP}|\sin\phi \tag{2}$$

$$|V_{IND}|\sin\theta = R_{REP}|I_{REP}|\sin\phi \tag{3}$$

where ω is the angular frequency of the operating frequency of the ATAC, θ is the phase angle of V_{IND}, ϕ is the phase angle of I_{REP}.

Noticing that I_{REP} must be perpendicular to V_{ATAC}, ϕ must be 90° according to (3) if θ is in the range of 0°–180°, whereas ϕ must be −90° if θ is in the range of 180°–360°. Therefore, the repeater coil current I_{REP} takes the maximum amplitude by adjusting θ at either 90° or −90°. The appropriate choice of θ from 90° and −90° is dependent on the reactance of the repeater resonator because the root-mean-square value must take a positive value. Consequently, θ=90° should be chosen according to (2) if $L_{REP}-1/\omega^2 C_{REP}$ takes a positive value, whereas θ=−90° should be chosen if $L_{REP}-1/\omega^2 C_{REP}$ takes a negative value. (In the practical application, however, $L_{REP}-1/\omega^2 C_{REP}$ should preferably be designed to take a positive value for achieving the soft-switching of the ATAC, which requires ϕ to be 90° rather than −90°.)

According to (3), the operation when θ is adjusted to maximize $|I_{REP}|$ results in a simple equation that $|V_{IND}|=R_{REP}|I_{REP}|$. This equation is equivalent to the operation of the repeater resonator when the ATAC is disconnected and the resonant frequency of the repeater resonator is accurately adjusted at the operating frequency of the transmitter. Therefore, these results can be interpreted as that the ATAC can equivalently adjust the resonant frequency of the repeater resonator.

As seen above, the ATAC needs to control only θ, which is the phase angle between the voltage induction and the gating signal of the low-side power device of the ATAC, so that the amplitude of the repeater coil current takes the maximum value. Therefore, the dc voltage V_{AT} of the decoupling capacitor of the ATAC is automatically determined without control. This voltage when the repeater coil current is maximized is obtained from (1)–(3) as

$$V_{AT} = \frac{\pi}{\sqrt{2}}\omega\left|L_{REP} - \frac{1}{\omega^2 C_{REP}}\right||I_{REP}| = \frac{\pi}{\sqrt{2}}\omega\left|L_{REP} - \frac{1}{\omega^2 C_{REP}}\right|\frac{|V_{IND}|}{R_{REP}} \quad (4)$$

In the practical design of the controller of the ATAC, the direct adjustment of θ is difficult because the accurate sensing of the voltage induction is difficult. To overcome this difficulty, the phase angle between the gating signal of the ATAC and transmitter coil current can be adjusted instead of θ because the induction voltage V_{IND} must be always perpendicular to that of the transmitter coil current according to Faraday's law. Alternatively, the phase angle between the inverter output voltage and the gating signal of the ATAC can also be utilized if the operation of the RIC-WPT system is stable and therefore the phase angle between the voltage induction and the inverter output voltage can also be regarded to be stable.

These phase angles are beneficial in easier measurement than θ, although the measurement will need wireless communication of the phase angle from the transmitter to the repeater. Figure 2 also presents an example of the control diagram of the controller of the ATAC. In this RIC-WPT system, the controller of the inverter of the transmitter sends the gating signal of a switching power device of the inverter as a real-time wireless communication signal, e.g. the infrared on-off keying signal. The receiver of the ATAC controller in the repeater resonator receives this signal and generates the sawtooth wave with twice as high frequency as the received signal, as depicted in Fig. 3(c). This sawtooth wave is generated in synchronization with the rising and falling edge of the received signal. Then, this sawtooth wave is compared using a comparator with the dc voltage signal V_{shift}, which is determined by the controller and represents the phase shift from the received signal, to generate the phase-shifted square wave with twice as high frequency as the received signal, as depicted in Fig. 3(d). Based on this square wave, a new square wave with the half frequency, which is identical to the frequency of the received signal, is generated in synchronization with the rising edge of the original square wave. Finally, this new square wave is utilized as the gating signal for the low-side power device of the ATAC. (The high-side gate signal is also generated from the low-side gate signal.)

The resultant gating signal of the ATAC has the phase shift from the received signal depending on the dc voltage supplied to the comparator. Therefore, by adjusting this dc voltage, the value of the phase shift between the received signal and the gating signal of the ATAC can be adjusted by the controller. This dc voltage is determined by the microprocessor of the controller according to the hill-climbing algorithm so that the amplitude of the repeater coil current is maximized.

As seen above, the previous tuning system is highly dependent on the real-time wireless communication of the inverter's gating signal or transmitter coil current. However, this wireless communication is highly complicated and difficult for high-frequency applications, where the timing of the rising and falling edges of the signal should be accurately transferred without significant delay. In the preceding work, the infrared signal is utilized for this wireless communication because of little legal restriction. However, the infrared signal restricts the installation location of the repeater resonator due to the limit of the reachable area of the infrared signal. To overcome this difficulty, the improved tuning system is proposed in the subsequent section.

III. Proposed Resonant Frequency Tuning System

A. System Configuration

Based on the aforementioned previous tuning system, the proposed resonant frequency tuning system eliminates the wireless communication from the transmitter and generates the received signal internally from the repeater coil current. Figure 5 illustrates the circuit schematic and the control diagram of the proposed tuning system. (Similarly to the previous section, the receiver is omitted to simplify the discussion.)

In the RIC-WPT system with the proposed resonant frequency tuning system, the transmitter and the repeater are independent without wireless communication. The repeater is

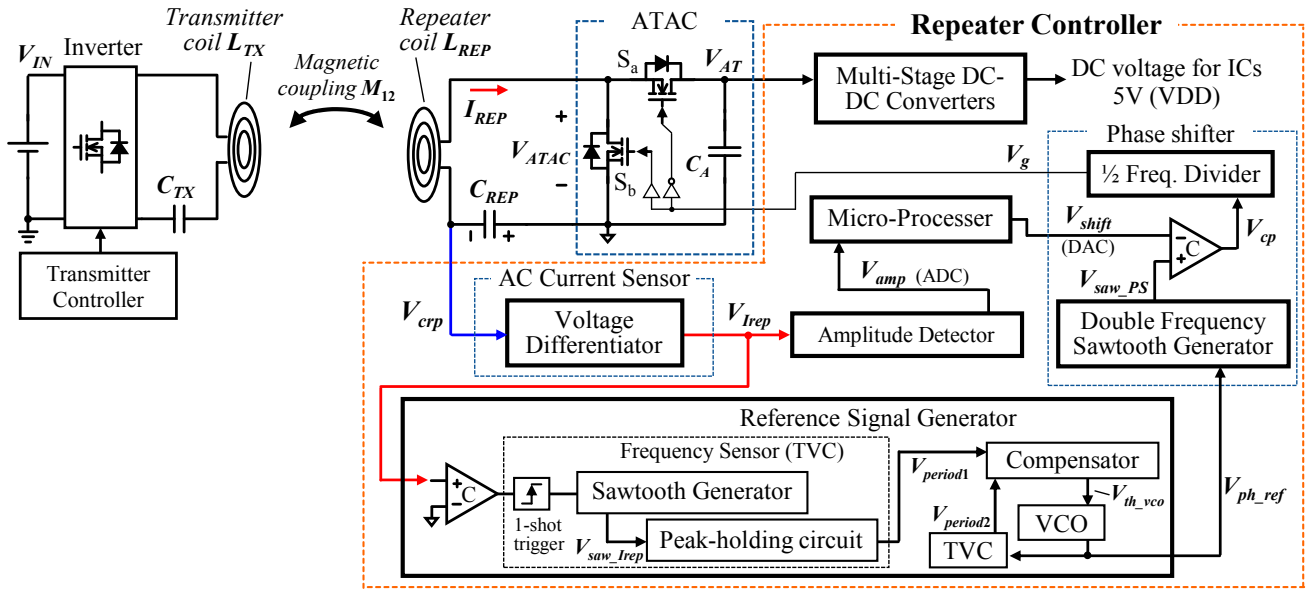

Fig. 5. Proposed resonant frequency tuning system for repeater resonator of resonant inductive coupling wireless power transfer system.

made of the series-connected repeater coil, resonant capacitor, and ATAC, similar to the previous tuning system. A DC-DC converter is attached to the decoupling capacitor of the ATAC for the power supply to the controller, which is also the same as the previous tuning system. However, the difference lies in the controller of the ATAC, which is surrounded by the dashed blue line.

In the previous tuning system, an operating waveform of the transmitter is adopted as the reference signal, which is phase-shifted by the ATAC controller of the repeater to generate the gating signal of the switching power devices of the ATAC. This is the reason why wireless communication is needed to provide the reference signal to the ATAC controller, which is installed in the repeater. However, in the proposed system, the reference signal itself is generated from the repeater coil current.

The proposed system generates the reference signal from the repeater coil current. According to the operating principle discussed in the previous section, the reference signal for the tuning system with the ATAC must satisfy the following two requirements: One is that the signal must have the same frequency as the voltage induction of the repeater resonator; the other is that the signal must have the stable phase difference with the voltage induction. The repeater coil current has the same frequency as the voltage induction. However, the phase angle of the repeater coil current lacks stability because the phase angle can be easily affected by the operation of the ATAC, i.e. the change in the phase shift angle θ and the dc voltage V_{AT}. Therefore, the proposed system generates the reference signal such that the signal has the same frequency as the repeater coil current but its phase angle is not directly affected by the operation of the ATAC.

For generating the reference signal, the proposed system firstly converts the frequency of the repeater current into the dc voltage $V_{period1}$ using the Time-Voltage Converter(TVC). At the same time, the frequency of the output of the Voltage-Controlled Oscillator (VCO) is also converted into the dc voltage $V_{preiod2}$. Then, these two dc voltages are compared at the compensator; the compensator adjusts the frequency of the VCO so that $V_{period2}$ takes the same value as $V_{period1}$. Finally, the output signal of the VCO is extracted and utilized as the reference signal.

As discussed above, the reference signal of the proposed tuning system has the same frequency as the repeater coil current. Furthermore, the reference signal is not directly affected by the operation of the ATAC and therefore the phase

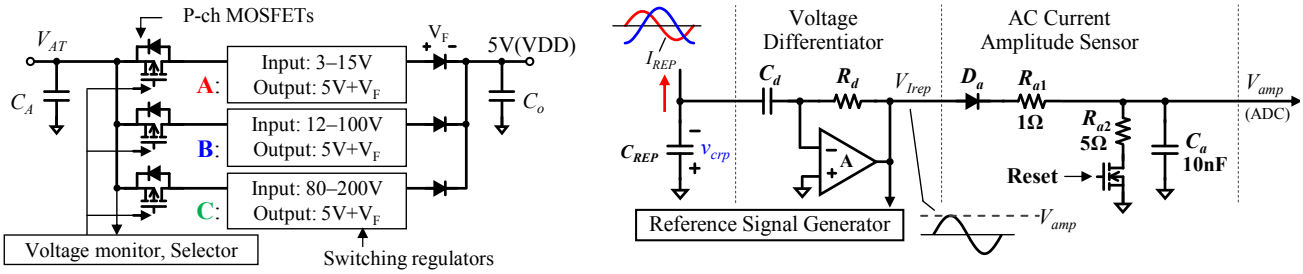

(a) Multi-stage DC-DC Converters

(b) AC Current Sensor and Amplitude Detector

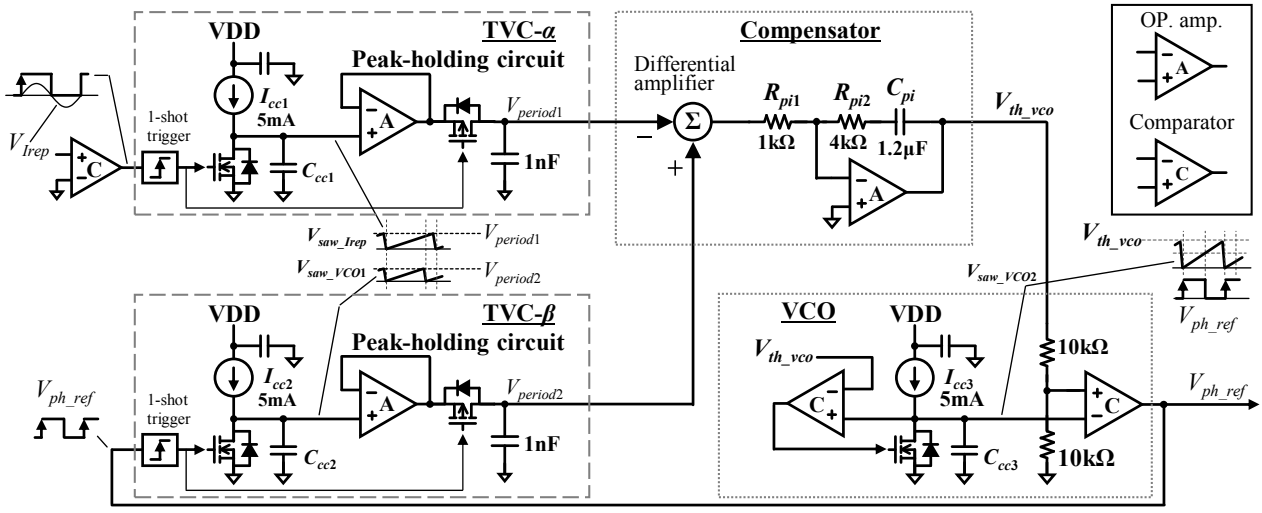

(c) Reference Signal Generator

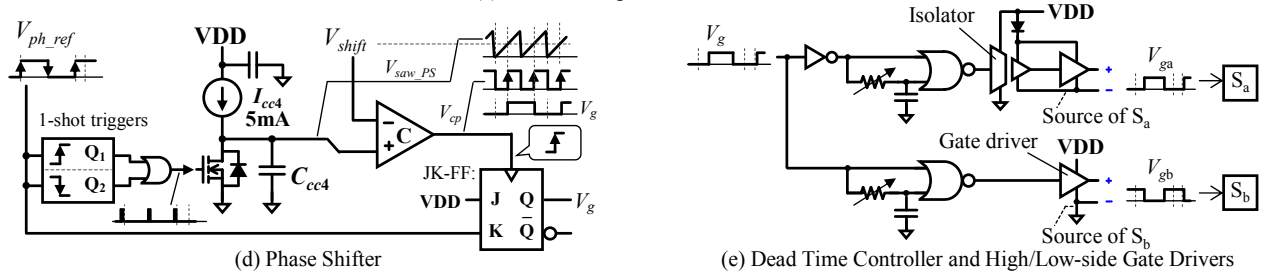

(d) Phase Shifter (e) Dead Time Controller and High/Low-side Gate Drivers

Fig. 6. Detail circuit diagram of control blocks of the control circuit of proposed resonant frequency tuning circuit.

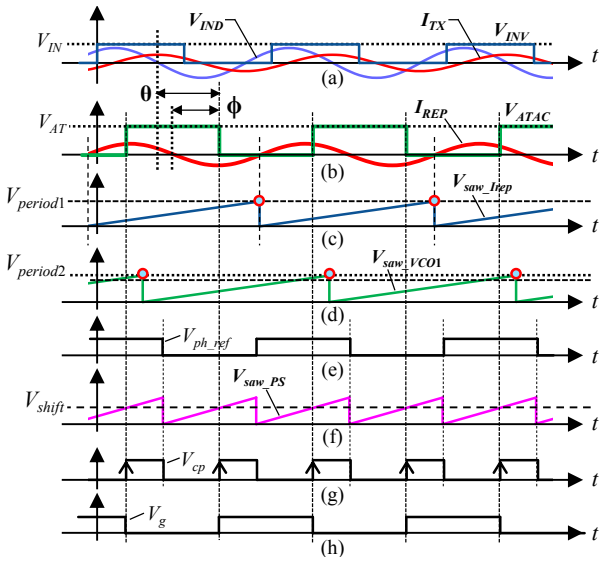

Fig. 7. Operating waveforms of the proposed automatic resonant frequency tuning system. (a) Inverter output voltage V_{INV} and transmitter coil current I_{TX}. (b) Repeater coil current I_{REP} and AC voltage generated by ATAC V_{ATAC}. (c) Sawtooth waveform V_{saw_Irep} in a TVC. (d) Sawtooth waveform V_{saw_VCO1} in another TVC. (e) Square wave V_{ph_ref} with constant phase. (f) Sawtooth waveform V_{saw_PS} with the twice as high frequency as the repeater current and the dc voltage V_{shift}. (g) Square wave V_{cp} with twice as high frequency as the repeater current comparing between V_{saw_PS} and V_{shift}. (h) Signal V_g for gating signals.

angle of the reference signal is more stable than the repeater coil current. Consequently, the reference signal can satisfy the aforementioned two requirements.

The gating signal of the ATAC is generated by applying the phase shift to the reference signal. The value of the phase shift is adjusted by the controller using the hill-climbing algorithm so that the amplitude of the repeater coil current is maximized, which is the same as the controller of the previous tuning system.

B. Circuit Design of Proposed Tuning System

Based on the system concept shown in the previous subsection, the practical circuit was designed according to the control diagram shown in Fig. 5. Figure 6 shows the practical circuit diagram of each control block in the proposed resonant frequency tuning system. Figure 7 shows the operating waveforms of the proposed resonant tuning system according to the circuit design of Fig. 6.

Figure 6(a) presents the DC-DC converter. Because the dc voltage V_{AT} stored in the decoupling capacitor of the ATAC varies greatly depending on the amplitude of the voltage induction and the resonance frequency deviation of the repeater resonator from the operating frequency of the inverter, the DC-DC converter that generates the dc power source for the ATAC controller must accept the wide range of the input voltage. For this purpose, the DC-DC converter is designed to be comprised of the parallel connection of plural switching regulators with a different range of input voltage. The active regulator is chosen by the microprocessor according to the dc voltage V_{AT}.

Figure 6(b) presents the ac current sensor and the amplitude detector. The ac current of the repeater coil is detected by differentiating the voltage of the resonance capacitor using an operational amplifier. Then, the output of the ac current sensor is applied with the rectifier of a diode D_a and a decoupling capacitor C_a to extract the peak value of the ac current, which is utilized as the amplitude. The resistor R_{a1} inhibits an in-rush current of C_a and R_{a2} adjusts the time constant in discharge from C_a.

Figure 6(c) presents the reference signal generator. The reference signal generator is a circuit classified as the Frequency Locked Loop Oscillator (FLL-OSC), made of two Time-Voltage Converters (TVCs), a VCO and a compensator.

At the start-up of the proposed tuning system, the ATAC controller starts generating the reference signal before the activation of the ATAC. The reference signal is generated by tuning the frequency of the VCO to that of the induced current in the repeater coil. For this purpose, the controller detects the ac current of the repeater coil and converts its frequency into the dc voltage $V_{period1}$ using the TVC. At the same time, the frequency of the output of the VCO is also converted into the dc voltage $V_{period2}$. These two dc voltages, i.e. $V_{period1}$ and $V_{period2}$, are compared by the compensator to adjust the output signal frequency of the VCO so that $V_{period2}$ takes the same value as $V_{period1}$. Finally, the output signal is utilized as the reference signal V_{ph_ref}.

The TVC is made of a 1-shot trigger, a sawtooth wave generator, and a peak-holding circuit. The 1-shot trigger is utilized to generate a short pulse signal that synchronizes the rising zero-cross timing of the repeater coil current. This pulse is fed to the sawtooth wave generator to generate the sawtooth wave that synchronizes the pulse. The sawtooth wave generator is made of a capacitor, a capacitor discharging circuit, which entirely discharges the capacitor at the pulse of the 1-shot trigger, and a charging circuit, which constantly charges the capacitor with the constant current. The sawtooth generator output the capacitor voltage, which forms the sawtooth wave as a result of charging and discharging. The voltage slope of the sawtooth wave is constant because of the constant current charging. Therefore, the maximum value of the sawtooth wave corresponds to the period of the input signal to the TVC. Finally, the maximum value of the sawtooth wave is detected by the peak-holding circuit and outputted as the output of the TVC. These two TVCs are designed to have the same Time-to-Voltage conversion ratio by accurately adjusting the constant current source of these two TVCs.

The compensator is made as a simple PI compensator with an operational amplifier. The function of this compensator is to compare the output voltages $V_{period1}$ and $V_{period2}$ of the two TVCs and outputs the voltage V_{th_vco}, according to the difference between $V_{period1}$ and $V_{period2}$. The time constant of the PI compensator is designed to be far greater than the resonant frequency so that the PI output is hardly affected by the slight phase disturbances of the repeater coil current caused by the transient fluctuation of the ATAC operation.

The VCO is made as a typical sawtooth generator, made of a capacitor, a capacitor discharging circuit, and a charging circuit, which constantly charges the capacitor with the constant current. The output voltage of the compensator is supplied to the input of the discharging circuit. The discharging circuit compares the capacitor voltage and the input voltage V_{th_vco} and discharges the capacitor if the capacitor voltage is greater than V_{th_vco}. Therefore, the lower input voltage results in the higher frequency of the sawtooth wave of the capacitor voltage. The capacitor voltage is supplied to the comparator that compares the capacitor voltage

TABLE I. SIMULATION SET-UP

Parameter	*Symbol*	Value
Self-inductance of the transmitter/repeater coil	L_{TX} L_{REP}	50 μH
Parasitic resistance of the transmitter/repeater coil	R_{TX} R_{REP}	0.5 Ω
Resonant capacitance of the transmitter/repeater resonator with +10% tolerance	C_{TX} C_{REP}	55.7 nF
Decaupling capacitance of ATAC	C_{A2}	3.3 μF
Coupling coefficiency between TX/REP coil	k_{12}	0.02
Mutual inductance	M_{12}	1.0 μH
Operating frequency of the RIC-WPT system	f_o	100 kHz
Resonant frequency of the transmitter/repeater resonators	f_{rTX} f_{rREP}	95.4 kHz
Control frequency of the hill-climbing algorithm	$f_{ctrl.}$	3.0 kHz
Input dc voltage of the half bridge inverter	V_{IN}	10 V
Amount of change of V_{shift} in one control cycle	δV_{shift}	0.028

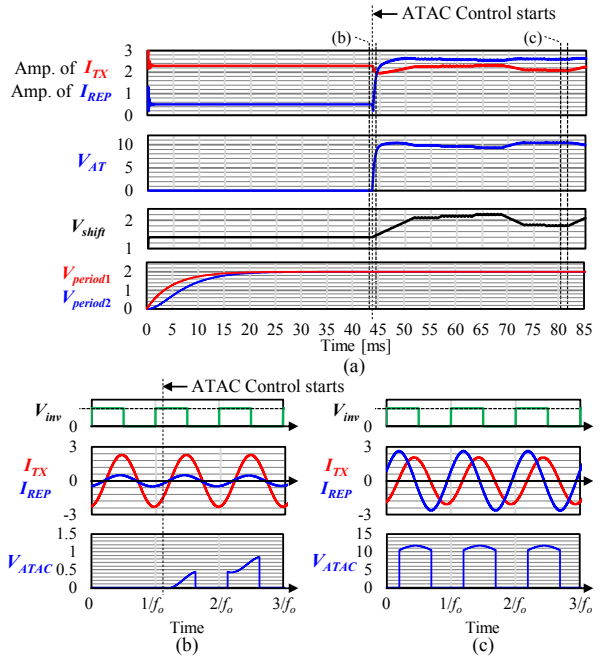

Fig. 8. Simulation waveforms of RIC-WPT system including repeater resonator with proposed resonant frequency tuning system. (a) Time transient waveforms from starting hill-climbing algorithm to steady state. (b) Immediately after control starts. (c) At steady state.

with the half of V_{th_vco}, thus transforming the sawtooth wave into the square wave with the 50% duty cycle.

Figure 6(d) presents the phase shifter. The reference signal V_{ph_ref}, generated by Fig. 6(c), is supplied to the phase shifter. As discussed in the previous subsection, the phase shift value can be changed, while maintaining the 50% duty ratio, by adjusting the dc voltage V_{shift}, which is determined and given by the microprocessor. The output signal of the phase shifter is supplied to the gate drivers of the ATAC.

The phase shifter is made of a double frequency sawtooth generator, a comparator, and a half-frequency divider, similarly to the previous tuning system. The double frequency sawtooth generator is made of a capacitor, a constant-current charging circuit, a discharging circuit, and a 1-shot trigger that outputs a pulse at both the rising and falling edge of the input square voltage signal. This pulse is supplied to the discharging circuit of the sawtooth generator, resulting in the sawtooth wave of the capacitor voltage with twice as large frequency as the input square wave voltage. The square wave voltage is supplied to the comparator that compares this voltage with the dc voltage V_{shift}, which is determined and supplied by the microprocessor. The output of the comparator is supplied to the JK flip-flop, which works as the half-frequency divider, thus outputting the phase-shifted square voltage waveform.

Finally, Fig. 6(e) presents the gate driving circuit of the ATAC. The phase-shifted square voltage waveform is input to the dead-time generator, which generates the gating signals of the ATAC. These gating signals are supplied to the gate driver, which drives the two switching power devices of the ATAC.

IV. SIMULATION

The simulation was conducted to confirm the operation of the proposed resonant frequency tuning system. Based on Figs. 5 and 6, the circuit simulation model of the RIC-WPT system with the proposed tuning system was constructed in the model space of the circuit simulator PSIM ver.11.1.2 (Powersim Inc.). This simulation also omitted the receiver resonator according to the same reason as in sections II and III.

The parameters of the constructed simulation model are shown in Table 1. In this simulation, the repeater resonator is designed to have a slight deviation of approximately 5% from the operating frequency, i.e. 100 kHz, of the inverter that supplies the ac power to the transmitting resonator. This deviation is reasonable in the practical RIC-WPT systems considering that commercial inductors and capacitors for high power applications commonly has the manufacturing tolerance of 10%.

After the start of the simulation, the tuning system starts operating the reference signal generator to synthesize the reference signal with the same frequency as the operating frequency. However, the proposed tuning system does not activate the ATAC for 44 ms after the start of the simulation. Therefore, this period can be regarded as the operation without the proposed tuning system. After 44 ms, the ATAC is activated, which corresponds to the operation with the proposed tuning system.

Figure 8(a) shows the overall operation of the simulated RIC-WPT system. As can be seen in the figure, $V_{period2}$ is controlled to be coincide with $V_{period1}$ within 20 ms from the start of the simulation, which indicates that the reference signal generator is generating the square wave signal with the same frequency as the operating frequency. After the 44 ms, where the ATAC starts its operation, the microprocessor outputs and adjusts the dc voltage V_{shift} to maximize the amplitude of the repeater coil current. As a result, the repeater coil current is increased to 2.62 Apeak approximately from 0.5 Apeak, which was observed before 44 ms. This amplitude of the repeater coil current is consistent with that of the RIC-WPT system whose resonance frequency of the repeater resonator is accurately identical to the operating frequency of the inverter, which is calculated as 2.69 Apeak.

Figures 8(b) and 8(c) are the operating waveforms of the RIC-WPT systems with the proposed tuning system at 44 ms, which is immediately after the start of the control, and at 80 ms, which corresponds to the steady operation, respectively. The output voltage of the ATAC increases gradually immediately after the start of control and almost in phase to the repeater coil current, which indicates that the decoupling

capacitor of the ATAC is gradually charged by the repeater coil current as expected by the operating principle of the ATAC. In the steady state, the phase of the repeater coil current was adjusted to be perpendicular to that of the ATAC output, which is consistent with the operation principle of the ATAC at the steady state because the ATAC is inserting the reactive voltage without receiving any active power. As a result of the appropriate phase adjustment of the ATAC output voltage, the repeater coil current is adjusted to have the phase in parallel to the transmitter coil current, which is also consistent with the operation when the resonance frequency of the repeater resonator was assumed to be accurately adjusted to the operating frequency of the inverter. Consequently, the proposed tuning system showed equivalent adjustment of the resonant frequency to the operating frequency successfully.

V. Conclusions

The RIC-WPT system with the repeater is a promising power supply method to small IoT devices distributed in a wide area. However, the resonant frequency of the repeater resonator is expected to deviate from the operating frequency of the transmitter due to the manufacturing tolerance and the aging effect in practical application, significantly deteriorating the power transfer capability. The previous study proposed a circuit system adjusting the resonant frequency of the repeater to the operating frequency, although this previously proposed system needs a wireless communication system, which will restrict the freedom of the installation location of the repeater.

To overcome this problem, this paper proposed a novel autonomous resonant frequency tuning system of the repeater without the need for wireless communication. The basic operation is tested by the simulation. The results supported the autonomous adjustment of the resonant frequency to the operating frequency without the wireless communication, implying the feasibility of the proposed resonant frequency tuning system for practical RIC-WPT systems.

References

[1] P. Pérez-Nicoli, A. Rodríguez-Esteva and F. Silveira, "Bidirectional analysis and design of RFID using an additional resonant coil to enhance read range," *IEEE Trans. Microw. Theory Techn.*, vol. 64, no. 7, pp. 2357-2367, July 2016.

[2] B. Couraud, T. Deleruyelle, R. Vauche, D. Flynn and S. N. Daskalakis, "A low complexity design framework for NFC-RFID inductive coupled antennas," *IEEE Access*, vol. 8, pp. 111074-111088, 2020.

[3] T. Yoshikawa and S. Saraya, "HEMS assisted by a sensor network having an efficient wireless power supply," *IEEE Trans. Magn.*, vol. 49, no. 3, pp. 974-977, March 2013.

[4] J. Zhu and B. Tao, "Simultaneous wireless power and data transmission over one pair of coils for sensor-integrated rotating cutter," *IEEE Access*, vol. 8, pp. 156954-156963, 2020

[5] K. Na, H. Jang, H. Ma and F. Bien, "Tracking optimal efficiency of magnetic resonance wireless power transfer system for biomedical capsule endoscopy," *IEEE Trans. Microw. Theory Techn.*, vol. 63, no. 1, pp. 295-304, Jan. 2015

[6] M. R. Basar, M. Y. Ahmad, J. Cho and F. Ibrahim, "An improved wearable resonant wireless power transfer system for biomedical capsule endoscope," *IEEE Trans. Ind. Electron.*, vol. 65, no. 10, pp. 7772-7781, Oct. 2018.

[7] Q. Xu, H. Wang, Z. Gao, Z. Mao, J. He and M. Sun, "A novel mat-based system for position-varying wireless power transfer to biomedical implants," *IEEE Trans. Magn.*, vol. 49, no. 8, pp. 4774-4779, Aug. 2013

[8] I. A. Mashhadi, M. Pahlevani, S. Hor, H. Pahlevani and E. Adib, "A new wireless power-transfer circuit for retinal prosthesis," *IEEE Trans. Power Electron.*, vol. 34, no. 7, pp. 6425-6439, July 2019.

[9] F. Liu, Y. Yang, Z. Ding, X. Chen, and R. M. Kannel, "Eliminating cross interference between multiple receivers to achieve targeted power distribution for a multi-frequency multi-load MCR WPT system," *IET Power Electron.*, vol. 11, no. 8, pp. 1321–1328, July 2018.

[10] L. Jiang and D. Costinett, "A high-efficiency GaN-based single-stage 6.78 MHz transmitter for wireless power transfer applications," *IEEE Trans. Power Electron.*, vol. 34, no. 8, pp. 7677–7692, Aug. 2019.

[11] U. Pratik, B. J. Varghese, A. Azad, and Z. Pantic, "Optimum design of decoupled concentric coils for operation in double-receiver wireless power transfer systems," *IEEE J. Emerg. Sel. Topics Power Electron.*, vol. 7, no. 3, pp. 1982–1998, Sept. 2019.

[12] R. Narayanamoorthi, A. V. Juliet, B. Chokkalingam, "Cross interference minimization and simultaneous wireless power transfer to multiple frequency loads using frequency bifurcation approach," *IEEE Trans. Power Electron.*, vol. 34, no. 11, pp. 10898–10909, Nov. 2019.

[13] M. Ishihara, K. Fujiki, K. Umetani, and E. Hiraki, "Automatic active compensation method of cross-coupling in multiple-receiver resonant inductive coupling wireless power transfer systems," in *Proc. IEEE Energy Convers. Congr. Expo.*, Baltimore, MD, USA, 2019, pp. 4584–4591.

[14] C.-S. Wang, G. A. Covic, O. H. Stielau, "Power transfer capability and bifurcation phenomena of loosely coupled inductive power transfer systems," *IEEE Trans. Ind. Electron.*, vol. 51, no. 1, pp. 148–157, Feb. 2004.

[15] R. Huang, B. Zhang, D. Qiu and Y. Zhang, "Frequency splitting phenomena of magnetic resonant coupling wireless power transfer," IEEE Trans. Magn., vol. 50, no. 11, pp. 1-4, Nov. 2014.

[16] A. Trigui, S. Hached, F. Mounaim, A. C. Ammari and M. Sawan, "Inductive power transfer system with self-calibrated primary resonant frequency," IEEE Trans. Power Electron., vol. 30, no. 11, pp. 6078-6087, Nov. 2015.

[17] M. Schormans, V. Valente and A. Demosthenous, "Practical inductive link design for biomedical wireless power transfer: a tutorial," IEEE Trans. Biomed. Circuits Syst., vol. 12, no. 5, pp. 1112-1130, Oct. 2018.

[18] M. Ishihara, S. Ohata, K. Fujiki, K. Umetani and E. Hiraki, "Improving Robustness Against Variation in Resonance Frequency for Repeater of Resonant Inductive Coupling Wireless Power Transfer Systems," 2018 20th European Conf. Power Electron. Appl. (EPE'18 ECCE Europe), 2018, pp. P.1-P.9.

[19] M. Ishihara, K. Umetani and E. Hiraki, "Impedance matching to maximize induced current in repeater of resonant inductive coupling wireless power transfer systems," 2018 IEEE Energy Conversion Congr. Expo. (ECCE), 2018, pp. 6194-620.

[20] K. Lee and S. H. Chae, "Power transfer efficiency analysis of intermediate-resonator for wireless power transfer," IEEE Trans. Power Electron., vol. 33, no. 3, pp. 2484-2493, Mar. 2018.

[21] Y. Endo and Y. Furukawa, "Proposal for a new resonance adjustment method in magnetically coupled resonance type wireless power transmission," 2012 IEEE MTT-S Intl. Microwave Workshop Series on Innovative Wireless Power Transmission: Tech., Syst., Appl., 2012, pp. 263-266

[22] J. Osawa, T. Isobe and H. Tadano, "Efficiency improvement of high frequency inverter for wireless power transfer system using a series reactive power compensator," 2017 IEEE 12th Intl. Conf. Power Electron. Drive Syst. (PEDS), 2017, pp. 992-998.

[23] R. Mai, Y. Liu, Y. Li, P. Yue, G. Cao and Z. He, "An active-rectifier-based maximum efficiency tracking method using an additional measurement coil for wireless power transfer," IEEE Trans. Power Electron., vol. 33, no. 1, pp. 716-728, Jan. 2018

[24] K. Kamaeguchi, K. Umetani, and E. Hiraki, "Application of automatic resonant frequency tuning circuit to induction heating system," Proc. European Conf. Power Electron. Appl. (EPE2018), 2018, pp. 1–9.

[25] K. Akihiro, F. Keita, U. Kazuhiro, E. Hiraki, "Resonant frequency tuning system for repeater resonator of resonant inductive coupling wireless power transfer," Proc. European Conf. Power Electron. Appl. (EPE2018), 2019, pp. 1–10.

[26] S. Mao, J. Zhang, K. Song, G. Wei, C. Zhu, "Wireless power transfer using a field-enhancing coil and a small-sized receiver with low coupling coefficient", IET Power Electron., vol. 9, no. 7, pp. 1546–1552, Jun. 2016.